

Role of interfacial mixing in giant magnetoresistance

V. S. Speriosu, J. P. Nozieres, and B. A. Gurney

IBM Research Division, Almaden Research Center, 650 Harry Road, San Jose, California 95120-6099

B. Dieny

*Laboratoire de Metallurgie Physique, Departement de Recherche Fondamentale sur la Matière Condensée/SP2M,
Centre d'Etudes Nucléaires de Grenoble, Boîte Postale 85,
38041 Grenoble CEDEX, France*

T. C. Huang and H. Lefakis

IBM Research Division, Almaden Research Center, 650 Harry Road, San Jose, California 95120-6099

(Received 14 December 1992)

We show that the giant magnetoresistance in sputtered Ni-Fe/Cu/Ni-Fe/Fe-Mn spin-valve structures is strongly reduced by the presence of compositionally intermixed regions at the NiFe/Cu interfaces. The ultrathin intermixed layers, which are not ferromagnetic, are centers of strong spin-independent scattering, thus reducing the flow of polarized electrons from one ferromagnetic layer to the other. Our results show that interfacial spin-independent scattering must be included in the theory of giant magnetoresistance.

Spin-dependent scattering (SDS) is widely accepted as the mechanism of giant magnetoresistance (GMR) in ferromagnet/nonferromagnet multilayers.¹⁻¹³ Depending on the material system, the SDS may have an interfacial^{1-5,7,11,13} or bulk^{6,9,10,13} character, or both.¹³ In bulk SDS the scattering ratio $\alpha \equiv \lambda^\uparrow/\lambda^\downarrow$, where λ^\uparrow (λ^\downarrow) is the electron mean free path of spin \uparrow (spin \downarrow) electrons, differs from unity everywhere within the ferromagnetic layer. For interfacial SDS, $\alpha \neq 1$ only within a narrow region at the ferromagnet/nonferromagnet interface. Thus bulk SDS is a property of the ferromagnet alone, while interfacial SDS is determined by the combination of metals forming the interface. For systems with interfacial SDS, such as Fe/Cr multilayers, the structure of the interface plays a dominant role. In particular, interface roughness increases the GMR in Fe/Cr multilayers,^{8,14} bolstering the view that the SDS is due to Cr impurities embedded in the Fe matrix along the interface.¹ In this paper we give a counter example where increasing the roughness (or compositional mixing) of the interface decreases rapidly the amplitude of the GMR. We choose Ni₈₀Fe₂₀ as the ferromagnet since, unlike for Co, Fe, or Ni, the GMR in NiFe is believed to be strongly dominated by bulk SDS.^{6,9,10,13} We show that in sputtered Ni-Fe/Cu/Ni-Fe/Fe-Mn spin valves the NiFe/Cu interfaces consist of ultrathin compositionally intermixed regions whose resistivity is much higher than that of Cu. The scattering in the nonferromagnetic, Cu-rich intermixed layers, which is not spin dependent, reduces the flow of electrons from one NiFe layer to the other, leading to reduced magnetoresistance. The thickness of the intermixed regions, measured by low-angle x-ray reflectivity and magnetometry, was systematically increased from 7 to 23 Å by sequential annealing up to 360°C. The annealing treatment led to a tenfold reduction in GMR with relatively little change in sheet resistance. By using spin-valve structures with essentially uncoupled ferromagnetic layers we avoid the ambiguities found in

antiparallel-coupled multilayers, where the magnitude of the observed magnetoresistance is influenced by current shunting in regions with parallel coupling.¹⁵ In contrast to multilayers, in spin valves the single-domain state of the magnetizations permits unambiguous measurement of the intrinsic GMR.¹⁶ Our results show that spin-independent scattering at interfaces, whose role has not been fully appreciated, must be included in the theoretical treatment of GMR.

Three series of spin-valve samples were prepared in a computer controlled dc magnetron sputtering system, with a base pressure of 5×10^{-8} Torr and an argon deposition pressure of 3 m Torr. The first series had the structure Si/50-Å Ta/ t_f Ni₈₀Fe₂₀/22.5-Å Cu/50-Å NiFe/110-Å Fe₅₀Mn₅₀/50-Å Ta, with $20 \text{ Å} \leq t_f \leq 600 \text{ Å}$. The second series comprised Si/50-Å Ta/75-Å NiFe/ t_{Cu} Cu/50-Å NiFe/110-Å FeMn/50-Å Ta, with $20 \text{ Å} \leq t_{Cu} \leq 400 \text{ Å}$. The third series consisted of Si/50-Å Ta/75-Å NiFe/25-Å Cu/ t_p NiFe/110-Å FeMn/50-Å Ta, with $20 \text{ Å} \leq t_p \leq 300 \text{ Å}$. The subscripts f and p , stand for free (i.e., layer whose moment is free to move in a magnetic field) and pinned (by exchange anisotropy due to FeMn), respectively. Magnetic and magnetotransport¹⁷ properties were measured at room temperature before and after sequential annealing steps at 240, 280, 320, and 360°C, each step lasting 6.5 hours. Annealing was carried out in a high vacuum furnace with pressure in the range of 10^{-7} Torr. During annealing a magnetic field was applied along the easy direction defined by exchange anisotropy. A companion sample, called the standard sample in what follows, with a structure comprising Si/50-Å Ta/75-Å NiFe/22.5-Å Cu/50-Å NiFe/110-Å FeMn/50-Å Ta, was subjected to the same annealing steps. Its structural properties, in particular the roughness or thickness of each interface, were measured by low-angle x-ray reflectivity, using a previously described procedure.¹⁸ Magnetic moment measurements were also

carried out on sandwiches comprising Si/50-Å Ta/ t NiFe/50-Å Ta, and Si/50-Å Ta/50-Å Cu/ t NiFe/50-Å Cu/50-Å Ta, with $5 \leq t \leq 75$ Å, subjected to the same annealing treatment.

To elucidate the magnetic behavior of the NiFe/Cu interfaces, the inset of Fig. 1 shows the saturation flux versus the thickness of NiFe in structures where the NiFe is sandwiched between Cu. The closed and open circles represent data for as-grown samples and after annealing at 320°C, respectively. Two features of the results are immediately apparent. First, the saturation flux is linear with layer thickness, with a slope giving a saturation magnetization equal to that of bulk NiFe. Second, the points are uniformly offset from the origin by a finite thickness which increases from 4 to 17 Å upon annealing. A dashed line going through the origin is also included to show what would be seen if all NiFe spins deposited contributed to the moment. The offset from the origin is due to the presence of nonferromagnetic layers (with zero moment at room temperature) located at the Cu/NiFe and NiFe/Cu interfaces. That these layers have zero, rather than just reduced, magnetization is shown, below a certain thickness, by the points with zero net moment. We are unable to separately identify the thickness of the nonferromagnetic layer for each interface, but we do not expect them to differ greatly. Thus we assign the thickness per interface, t_{nf} (NiFe/Cu), of the nonferromagnetic layer equal to one half of the offset. For as-deposited samples t_{nf} (NiFe/Cu) = 2.0 ± 0.16 Å. Annealing at 320°C increases t_{nf} (NiFe/Cu) to 8.4 ± 1 Å, without changing the saturation magnetization within the bulk of the layer. Measurements carried out on Si/50-Å Ta/ t NiFe/50-Å Ta, yield similar results regarding the slope of the saturation flux versus t , with t_{nf} (NiFe/Ta) = 6.4 ± 1 Å in as-deposited samples. Similarly, for the as-deposited Ta/NiFe/Cu structure in a full spin valve, the measured sum of the nonferromagnetic layers is 7.8 ± 2 Å, in very good agreement with t_{nf} (NiFe/Cu) + t_{nf} (NiFe/Ta) = 8.4 ± 1 Å. The physical origin of the nonferromagnetic layers at interfaces is either due to changes in the electronic band structure caused by proximity effects or, more like-

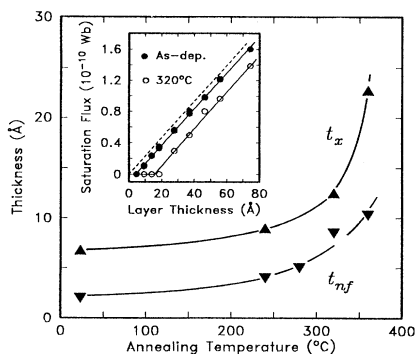


FIG. 1. Thickness of the nonferromagnetic layer per NiFe/Cu interface, t_{nf} (▼), vs annealing temperature. The ▲'s are the thicknesses t_x of the NiFe/Cu interface measured by x-ray low-angle reflectivity. Inset: magnetic saturation flux vs thickness t in sandwiches of the form Si/50-Å Ta/50-Å Cu/ t NiFe/50-Å Cu/50-Å Ta, for as-deposited samples (●) and after annealing at 320°C (○).

ly, to compositional gradients across the interfaces. In bulk Ni, the addition of 35% Cu or 20% Ta produces paramagnetic alloys with zero magnetization at room temperature.^{19,20}

Figure 1 shows the thickness t_{nf} (NiFe/Cu) of the nonferromagnetic layer per NiFe/Cu interface versus annealing temperature. Also shown is the thicknesses, t_x , of the NiFe/Cu interfaces in the standard spin-valve structure, measured by low-angle x-ray reflectivity. The thicknesses t_x for NiFe/Cu and Cu/NiFe interfaces were within 10% of each other. We note that the x-ray results give a measure of the total thickness of the intermixed region. In contrast, the thickness of the nonferromagnetic layer includes only those portions of the NiFe layer for which the Cu concentration exceeds a threshold value (i.e., $\approx 50\%$). Consequently it is not surprising that the thickness of the interface obtained by x-ray reflectivity is roughly twice as large as the thickness of the nonferromagnetic layer. The present x-ray measurements do not contain information on the lateral wavelength of the roughness,¹⁸ i.e., they do not distinguish between roughness on an atomic scale (intermixing) and deviations from flatness with a wavelength of, say 1000 Å. However the close correspondence between the thicknesses obtained by x-ray reflectivity and by magnetometry strongly suggests that the roughness is on an atomic scale. In Fig. 1 both thicknesses are finite for as-grown samples and increase monotonically with annealing, reaching t_{nf} (NiFe/Cu) = 10.3 ± 1.5 Å and t_x (NiFe/Cu) = 22.6 ± 1 Å at 360°C. Interface widths and thicknesses of the nonferromagnetic layers were also measured at each interface of the standard structure.²¹ Although the trends are similar, we do not discuss them in detail since these interfaces are far away from the regions where the exchange of electrons between the two NiFe layers leads to GMR.

Figure 2 shows the magnetoresistance $\Delta R/R$ versus the thickness t_f of the free NiFe layer for various annealing temperatures. The data were fitted by functions of the form $A R_{\square} [1 - \exp(-t_f/t_0)]$, where A is the characteristic spin-valve amplitude, R_{\square} is the sheet resistance and, at 0 K, t_0 is linearly related to the longer of the two mean free paths in NiFe.^{9,10,12} At the two highest annealing temperatures, for samples with large t_f , the exchange anisotropy field provided by the FeMn layer de-

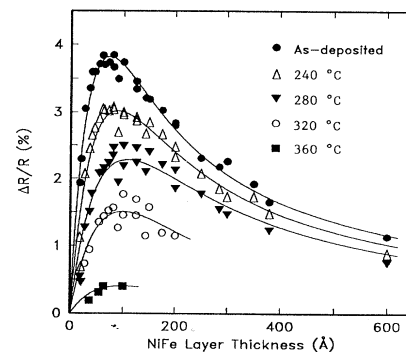


FIG. 2. Magnetoresistance $\Delta R/R$ for various annealing temperatures vs thickness t_f in Si/50-Å Ta/ t_f NiFe/22.5-Å Cu/50-Å NiFe/110-Å FeMn/50-Å Ta structures.

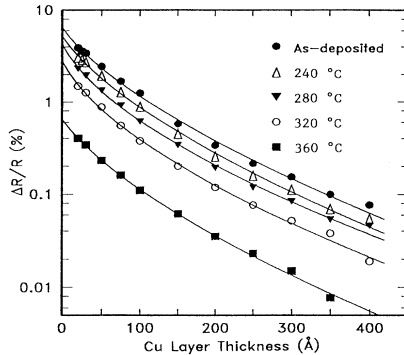


FIG. 3. $\Delta R/R$ for various annealing temperatures vs thickness t_{Cu} in Si/50-Å Ta/75-Å NiFe/ t_{Cu} Cu/50-Å NiFe/110-Å FeMn/50-Å Ta structures.

creased too much to permit independent switching of the magnetizations and thus any measurement of the GMR. We note that for all values of t_f , $\Delta R/R$ decreases with each annealing step. After annealing at 360 °C the peak $\Delta R/R$ is an order of magnitude smaller than as deposited. This is in sharp contrast to Fe/Cr multilayers⁸ where annealing at 300 °C for 1 hour *doubled* the GMR. The results for the series of samples with varying pinned NiFe layer thickness, t_p , were very similar to those of Fig. 2.

Figure 3 shows $\Delta R/R$ versus the thickness of the Cu layer. The data were fitted by functions of the form $C[\exp(-t_{\text{Cu}}/\lambda_{\perp})]/(t_{\text{Cu}} + t_s)$, where λ_{\perp} is related to the electron mean free path in the direction perpendicular to the interface^{10,12,22} and t_s is the equivalent Cu shunting thickness of the rest of the layered structure. Thus while t_{Cu} in the denominator represents the shunting of the current within the Cu layer,¹¹ t_s accounts for shunting by the rest of the structure. The $\exp(-t_{\text{Cu}}/\lambda_{\perp})$ term represents the reduction of GMR due to scattering within the Cu layer while C contains both the intrinsic GMR amplitude²² and any effects of the intermixed regions. For the as-deposited samples, $C = (254 \pm 36)\%$, $\lambda_{\perp} = 187 \pm 15$ Å, and $t_s = 35 \pm 9$ Å. Figure 4 presents the variation with annealing temperature of the parameters C , λ_{\perp} , and t_s , normalized to their respective values before annealing. While λ_{\perp} and t_s show only a slight decrease

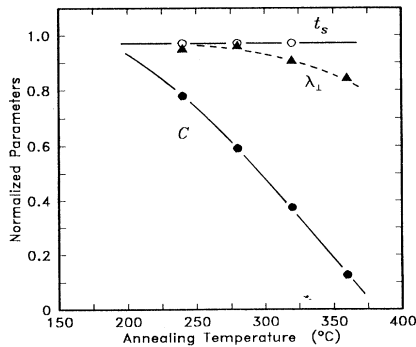


FIG. 4. Variation with annealing temperature of the fit parameters obtained from Fig. 3 and described in the text, normalized to their respective values before annealing.

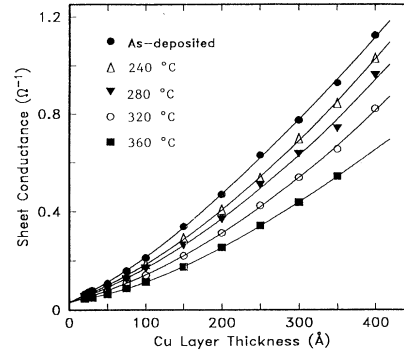


FIG. 5. Sheet conductance for various annealing temperatures vs thickness t_{Cu} in Si/50-Å Ta/75-Å NiFe/ t_{Cu} Cu/50-Å NiFe/110-Å FeMn/50-Å Ta structures.

with annealing, C decreases rapidly, approaching zero at 375°. The sharp decrease in C points to increasing spin-independent or to spin-flip scattering within the intermixed regions at the NiFe/Cu interfaces.

Figure 5 shows the sheet conductance G versus Cu layer thickness. Note that while the GMR drops by an order of magnitude with annealing, the sheet conductance decreases by only $\approx 50\%$. A similar trend was reported in annealed NiFe/Cu multilayers where the increased resistivity was attributed to increased dissolution of the NiFe and Cu layers.²³ To first order, the conductance of the spin-valve structure is given by $G \approx G_{\text{rest}} + t/\rho$ where t and ρ are the thickness and resistivity, respectively, of the layer in question, and G_{rest} is the conductance of the rest of the structure.⁹ For $t \gg \lambda$, the above relation becomes an equality, while for $t \lesssim \lambda$ finite-size effects lead to more complicated behavior.¹² We define an effective resistivity $\rho_{\text{eff}} = (dG/dt)^{-1}$, keeping in mind that for small thicknesses ρ_{eff} is determined not only by the mean free path within the layer but also by the mean free paths in the adjacent layers. In particular, for small Cu thickness ρ_{eff} includes contributions from the intermixed regions at the Cu/NiFe interfaces. We discuss the values of ρ_{eff} for small (20–30 Å) and large (400–600 Å) thicknesses (for bulk Cu $\lambda \approx 300$ Å at room temperature). For NiFe prior to annealing, these are 30 and 25 $\mu\Omega$ cm, while for Cu the corresponding quantities are 6.4 and 2.8 $\mu\Omega$ cm, respectively.

Figure 6 shows effective resistivities of the Cu and NiFe layers versus annealing temperature, normalized to as-deposited values. For large thickness ρ_{eff} changes relatively little. In thick permalloy the slight decrease is due to grain growth, while in thick Cu the increase is likely due to diffusion of Ni and Fe.²⁴ As for all pure noble metals, the resistivity of Cu increases rapidly with small impurity concentrations. In our samples, this behavior stands out at small Cu layer thickness, where the effective resistivity increases by more than a factor of 4. A similar, but less pronounced trend is seen for thin NiFe. In both cases the rise in ρ_{eff} is due to the increased thickness of the intermixed regions at the NiFe/Cu interfaces. Since the intermixed regions on the Cu side of the interfaces are Cu rich, they are not ferromagnetic, at least at

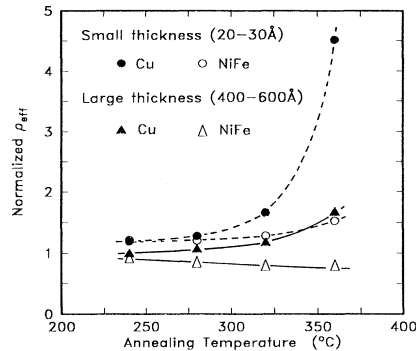


FIG. 6. Variation with annealing temperature of the effective resistivities ρ_{eff} , normalized to their respective values before annealing.

room temperature. Thus the scattering of the electrons in these regions cannot be spin dependent. Instead the scattering reduces the flux of electrons traversing the spacer from one NiFe layer to the other. Significant spin-flip scattering is also expected if the nonferromagnetic layers are paramagnetic. The resulting decrease in GMR is large, as demonstrated by the results of Figs. 2 and 3. Increasing the thickness of the intermixed region from 7 to 23 Å leads to a tenfold drop in $\Delta R/R$, even though R is relatively unchanged. It is worth noting that even in as-grown samples the thickness of the intermixed region is significant. This implies that the GMR in as-grown samples is already reduced from a higher value it would have had in the absence of intermixing. Using the data of Figs. 1 and 2, we estimate that for zero thickness of the intermixed layer, the GMR of the as-deposited structures would be 50% higher. Consequently the comparison of the amplitude of GMR in different systems, such as NiFe/Cu and Co/Cu, must take into account the different thicknesses of the nonferromagnetic interfacial layers. Our measurements show that $t_{\text{NF}}(\text{Co/Cu}) = 1.0 \pm 0.2$ Å at room temperature, a value *half* that for NiFe/Cu. This accounts for at least a portion of the larger GMR seen in Co/Cu versus NiFe/Cu.⁹ Differences in the deposition method may also lead to

differences in the amount of intermixing and therefore in the amplitude of the GMR.

In contrast to the present results, in Fe/Cr multilayers interface mixing leads to increased GMR, at least up to a point.^{8,14} The difference is due to the different nature of the spin-dependent scattering (SDS) in the Fe/Cr system versus that in NiFe/Cu. In Fe/Cr the SDS is interfacial,^{1-5,7} meaning that the difference in scattering rates of the spin \uparrow and spin \downarrow electrons is confined to the region of the interface. In the NiFe/Cu system the SDS is bulk, i.e., the difference in scattering rates is a property of NiFe, rather than that of the NiFe/Cu interface.^{6,9,10,13} The intermixing of Cu and NiFe, rather than increasing the difference in scattering rates, *decreases* this difference through spin-independent scattering.

In summary we have shown that compositional intermixing at the interfaces of NiFe/Cu spin valves creates ultrathin layers with no magnetic moment at room temperature and with a resistivity much higher than that of Cu. The scattering within these layers is not spin dependent and may include spin-flip scattering. Thus the intermixed layers decrease the flow of electrons across the spacer, effectively isolating the ferromagnetic layers from each other. As expected from the presence of such interfacial layers, which we have just demonstrated, the amplitude of the giant magnetoresistance is reduced. Our results shed new light on the role of interfaces in GMR: rather than always being the location of spin-dependent scattering (and thus at the origin of GMR), we have shown that spin-independent scattering occurs at the interfaces of at least one ferromagnet/nonferromagnet combination, leading to a sharp reduction of GMR. In general the nature and location of scattering depends on the materials used and on the state of intermixing at the interface. In particular spin-independent scattering within nonferromagnetic alloys at interfaces must be taken into account in theories of giant magnetoresistance as well as in comparisons of GMR in different systems where the thickness of the nonferromagnetic layers may be different.

We thank Dennis R. Wilhoit and Omar U. Need for expert technical assistance.

¹M. N. Baibich *et al.*, Phys. Rev. Lett. **61**, 2472 (1988).

²G. Binasch *et al.*, Phys. Rev. B **39**, 4828 (1989).

³R. E. Camley and J. Barnas, Phys. Rev. Lett. **64**, 664 (1989).

⁴P. M. Levy, S. Zhang, and A. Fert, Phys. Rev. Lett. **65**, 1643 (1990).

⁵B. A. Gurney *et al.*, IEEE Trans. Magn. **MAG-26**, 2747 (1990).

⁶B. Dieny *et al.*, Phys. Rev. B **43**, 1297 (1991).

⁷P. Baumgart *et al.*, J. Appl. Phys. **69**, 4792 (1991).

⁸F. Petroff *et al.*, J. Magn. Magn. Mater. **93**, 95 (1991).

⁹B. Dieny *et al.*, Phys. Rev. B **45**, 806 (1992).

¹⁰B. Dieny, Europhys. Lett. **17**, 261 (1992).

¹¹S. S. P. Parkin (unpublished).

¹²B. Dieny, J. Phys. Condens. Matter **4**, 8009 (1992).

¹³B. Dieny *et al.* (unpublished).

¹⁴E. F. Fullerton *et al.*, Phys. Rev. Lett. **68**, 859 (1992).

¹⁵A. Fert *et al.* (unpublished).

¹⁶V. S. Speriosu *et al.*, Phys. Rev. B **44**, 5358 (1991).

¹⁷Because in spin valves the magnetoresistance is measured for complete, single-domain, parallel and antiparallel alignment, the conventional anisotropic magnetoresistance does not contribute to the signal, regardless of the direction of the current.

¹⁸T. C. Huang *et al.*, Appl. Phys. Lett. **60**, 1573 (1992).

¹⁹R. M. Bozorth, *Ferromagnetism* (Van Nostrand Reinhold, New York, 1957).

²⁰B. D. Cullity, *Introduction to Magnetic Materials* (Addison-Wesley, New York, 1972).

²¹J. P. Nozieres *et al.* (unpublished).

²²B. Dieny, V. S. Speriosu, and S. Metin, Europhys. Lett. **15**, 227 (1991).

²³S. S. P. Parkin, Appl. Phys. Lett. **60**, 512 (1992).

²⁴H. Lefakis, J. F. Cain, and P. S. Ho, Thin Solid Films **101**, 173 (1984); M. Kitada, H. Yamamoto, and H. Tsuchiya, *ibid.* **122**, 173 (1984).